NeuroImage 59 (2012) 2824–2830

Contents lists available at SciVerse ScienceDirect

NeuroImage

journal homepage: www.elsevier.com/locate/ynimg

Biological motion processing: The left cerebellum communicates with the right superior temporal sulcus

Arseny A. Sokolov [a,b,*], Michael Erb [c], Alireza Gharabaghi [a,d], Wolfgang Grodd [e], Marcos S. Tatagiba [a], Marina A. Pavlova [b,f]

[a] Department of Neurosurgery, University of Tübingen Medical School, Germany
[b] Developmental Cognitive and Social Neuroscience Unit, Department of Pediatric Neurology and Child Development, Children's Hospital, University of Tübingen Medical School, Germany
[c] Department of Neuroimaging and MR Physics, University of Tübingen Medical School, Germany
[d] Neuroprosthetics Research Group, Werner Reichardt Centre for Integrative Neuroscience, University of Tübingen Medical School, Germany
[e] Department of Psychiatry, Psychotherapy and Psychosomatics, University Hospital Aachen, Germany
[f] Institute of Medical Psychology and Behavioral Neurobiology, MEG Center, University of Tübingen Medical School, Germany

ARTICLE INFO

Article history:
Received 9 May 2011
Revised 21 July 2011
Accepted 15 August 2011
Available online 13 October 2011

Keywords:
Biological motion perception
Cerebellum
Functional magnetic resonance imaging (fMRI)
Superior temporal sulcus (STS)
Connectivity

ABSTRACT

The cerebellum is thought to be engaged not only in motor control, but also in the neural network dedicated to visual processing of body motion. However, the pattern of connectivity within this network, in particular, between the cortical circuitry for observation of others' actions and the cerebellum remains largely unknown. By combining functional magnetic resonance imaging (fMRI) with functional connectivity analysis and dynamic causal modelling (DCM), we assessed cerebro-cerebellar connectivity during a visual perceptual task with point-light displays depicting human locomotion. In the left lateral cerebellum, regions in the lobules Crus I and VIIB exhibited increased fMRI response to biological motion. The outcome of the connectivity analyses delivered the first evidence for reciprocal communication between the left lateral cerebellum and the right posterior superior temporal sulcus (STS). Through communication with the right posterior STS that is a key node not only for biological motion perception but also for social interaction and visual tasks on theory of mind, the left cerebellum might be involved in a wide range of social cognitive functions.

Introduction

Veridical visual perception and understanding of others' actions are indispensable in a variety of daily-life situations ranging from motor learning to complex social interaction and non-verbal communication. Brain imaging, electrophysiology and lesion studies help to identify the neural network engaged in visual processing of biological motion. The findings indicate involvement of several brain regions, including portions of the frontal (Saygin et al., 2004) and parietal cortices (Bonda et al., 1996; Grèzes et al., 2001; Pavlova et al., 2004; Vaina et al., 2001), the fusiform gyrus (Gobbini et al., 2007; Grossman and Blake, 2002; Peelen et al., 2006; Vaina et al., 2001) and, in particular, the posterior superior temporal sulcus, pSTS (Beauchamp et al., 2002, 2003; Gobbini et al., 2007; Grossman and Blake, 2002; Pelphrey et al., 2003; Peuskens et al., 2005; Puce and Perrett, 2003; Saygin et al., 2004), mainly in the right hemisphere.

Deficient visual perception of body motion is observed in individuals with neuropsychiatric conditions associated with impairments in social cognition, such as autistic spectrum disorders, ASD (Blake et al., 2003; Klin et al., 2009; Koldewyn et al., 2010) and schizophrenia (Kim et al., 2005). Brain imaging points to reduced brain response to human body motion in the right temporal cortex in adolescents born prematurely with early white matter lesions, periventricular leukomalacia (Pavlova et al., 2009) as well as in autistic children (Kaiser et al., 2010). Veridical perception of body motion requires intact communication within the distributed brain network specialized for biological motion processing (Pavlova et al., 2007). Information flow, however, is primarily considered to be limited to cortico-cortical connections, and engagement of brain structures beyond the cerebral cortex such as the cerebellum has not yet been properly addressed. Since the first brain imaging data on cerebellar engagement in language processing (Petersen et al., 1989), the traditional view on the role of the cerebellum has progressively shifted from contributions to motor control and skilled motor behavior to a broad involvement in higher cognitive processing (for review, see Strick et al., 2009). Recent lesion data in patients with cerebellar tumors emphasize importance of left lateral cerebellar integrity for intact biological motion perception (Sokolov et al., 2010). However, a few previous brain imaging, functional magnetic resonance imaging (fMRI) and positron emission tomography (PET), studies produced controversial results in regard to topography of cerebellar activation in response to

* Corresponding author at: Department of Neurosurgery, University of Tübingen Medical School, Hoppe Seyler Strasse 3, DE-72076 Tübingen, Germany. Fax +49 7071 295253.
E-mail address: arseny.sokolov@med.uni-tuebingen.de (A.A. Sokolov).

1053-8119/$ – see front matter © 2011 Elsevier Inc. All rights reserved.
doi:10.1016/j.neuroimage.2011.08.039

biological motion (Bonda et al., 1996; Grossman et al., 2000; Ptito et al., 2003; Vaina et al., 2001). It remains unclear which cerebellar substructures are engaged and how the cerebellum may interact with the cortical circuitry underpinning action observation.

Findings on neuroanatomical architecture in non-human primates suggest that the parieto-temporal cortices might have contralateral connections with the cerebellum (Brodal, 1978; Clower et al., 2001; Dum and Strick, 2003; Glickstein et al., 1985; Schmahmann and Pandya, 1991). As the right parieto-temporal areas are of particular importance for visual processing of biological motion (Beauchamp et al., 2002, 2003; Grossman and Blake, 2002; Pavlova et al., 2004, 2009; Pelphrey et al., 2003), we expected that the left cerebellum might be engaged in the neural network dedicated to body motion processing. In the present work, we used event-related fMRI to measure blood oxygen level dependent (BOLD) signal while healthy volunteers performed a one-back repetition task with displays portraying human locomotion. In order to separate information revealed by motion from other cues, we took advantage of point-light biological motion consisting of a set of dots on the main joints of an otherwise invisible human body. Point-light animations represented either a human walker moving as if on a treadmill with no net translation or its scrambled version for which spatial positions of dots were randomly rearranged on the screen (Fig. 1). To elucidate cerebellar engagement in the neural network underpinning biological motion processing, functional and effective connectivity were assessed by using seed-voxel regression and dynamic causal modelling (DCM).

Material and methods

Participants

Thirteen healthy, right-handed, male volunteers (mean age 28.2 ± 6.3 years) with normal or corrected-to-normal vision were enrolled in the study. None had a history of neurological or psychiatric disorders, head injuries, or medication for anxiety or depression. They were naïve as to the purpose of the study and did not possess previous experience with point-light biological motion stimuli. Informed written consent was obtained in accordance with the requirements of the local Ethical Committee of the University of Tübingen Medical School.

Biological motion stimuli and task

Participants were presented with a set of 100 point-light biological motion stimuli of two types. One type of stimuli portrayed a canonical point-light walker, and consisted of 11 dots placed on the head and main joints (ankles, shoulder, etc.) of an otherwise invisible human figure (Fig. 1A). The point-light walker was seen facing right and moving as if on a treadmill without translation (see Supplementary Materials for Video). A gait cycle was completed in 62 frames with frame duration of 20 ms, resulting in a walking speed of about 48 cycles per minute. The other type of stimuli was a scrambled walker, for which the spatial positions of dots were randomly rearranged on the screen so that the display lacked the implicit coherent structure of a canonical one (Fig. 1B). The motion of each dot of the scrambled display was identical to the motion of one of the dots defining the canonical figure. The size, luminance, and phase relations of the dots also remained unchanged. The animations were computer generated by using Cutting's algorithm (Cutting, 1978), and displayed by using the software Presentation (Neurobehavioral Systems Inc., Albany, CA, USA). Each stimulus was presented for 1000 ms. The animations were projected on a screen outside the MRI scanner and subtended a visual angle of 4° in height and 2.5° in width. Participants viewed them through a tilted mirror located on the head coil. Participants performed a one-back repetition task, signaling a repeated stimulus of each type (canonical or scrambled) by a button press with their right index finger. Similar stimulation and task were used in previous magnetoencephalographic work (Pavlova et al., 2004). Here, they were adapted for fMRI.

Data acquisition and analysis

MRI recordings were obtained with a 3T scanner (TimTrio, Siemens Medical Solutions, Erlangen, Germany; 12 channel head coil). In all participants, the MRI acquisition frames were carefully positioned covering

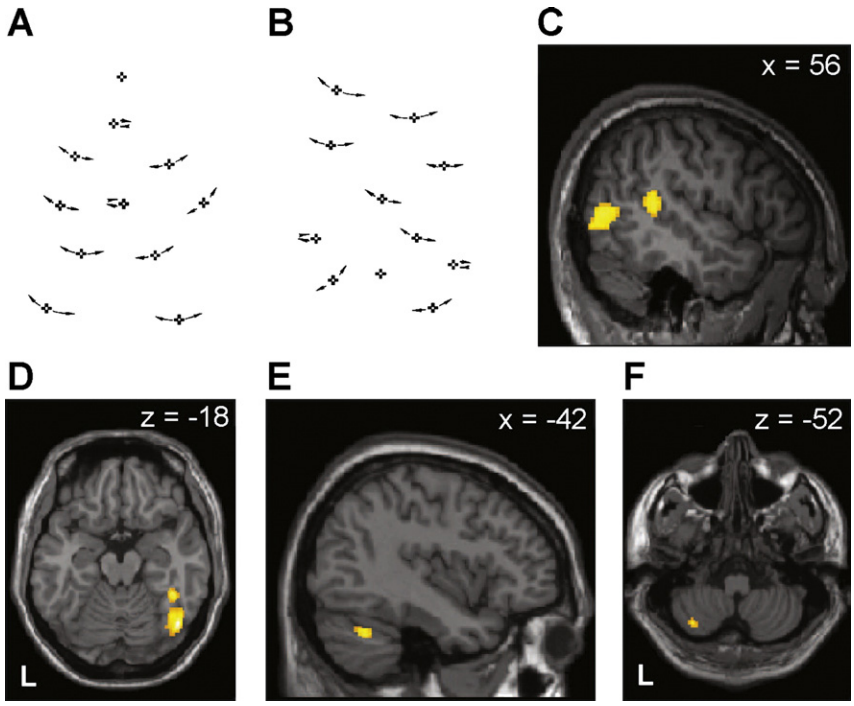

Fig. 1. Schematic illustration of point-light stimuli and fMRI brain activation in response to biological motion. Participants viewed either (A) a canonical point-light human figure walking as if on a treadmill (from Pavlova et al., 2003), or (B) its spatially scrambled version (from Pavlova et al., 2004), consisting of eleven moving dots each. The whole-brain fMRI analysis reveals robust activity for biological motion as compared to scrambled motion ($p<0.05$, corrected for multiple comparisons) in (C) the right posterior superior temporal sulcus (pSTS), the right middle temporal cortex, (D) the right fusiform gyrus, and the left cerebellar lobules (E) Crus I and (F) VIIB. Activation is overlaid on the MNI T1-template. Slice positions are provided in MNI space.

the most caudal cerebellar regions. Initially, a 3D T1-weighted magnetization-prepared rapid gradient echo imaging data set (MPRAGE; 176 sagittal slices, TR = 2300 ms, TE = 2.92 ms, TI = 1100 ms, voxel size = 1 × 1 × 1 mm³) was acquired as anatomical reference. Subsequently, a field map was recorded for later correction of magnetic field inhomogeneity. Echo-planar imaging sequences (EPI; 210 volumes, 36 axial slices, TR = 2500 ms, TE = 35 ms, in-plane resolution 3 × 3 mm², slice thickness = 3 mm, 1 mm gap) measuring the BOLD signal were obtained during the experimental task. We used an event-related design with total session duration of 525 s. An initial baseline fixation period (25 s) was followed by five event-related blocks (75 s each) that were interleaved with five baseline epochs (25 s each). An event-related block included 20 trials, with both types of stimuli being equally represented. The stimulus order was pseudo-randomized to optimize the estimation efficiency. Stimulus onset intervals were jittered in steps of 500 ms from 2500 to 5000 ms that allowed for increased temporal resolution, and thus better estimation of the event-related response function.

The data were pre-processed and analyzed by using Statistical Parametric Mapping (SPM8, Wellcome Institute of Cognitive Neuroscience, London, UK, http://www.fil.ion.ucl.ac.uk/spm) in Matlab R2008b (MathWorks Inc. Sherbon, MA, USA). In each individual data set, the T1-weighted anatomical reference image was initially aligned with the AC–PC plane and the resulting transformation matrix was applied to the field map and EPI images. Subsequently, acquisition time delay and movement artifacts were corrected by using SPM algorithms for slice timing and realignment. EPI images were unwarped based on the estimated field map data. The resulting images were then co-registered to the anatomical reference image. The unified segmentation procedure of SPM was used to determine the parameters for subsequent normalization to MNI space. As a final pre-processing step, the normalized data were smoothed with an isotropic Gaussian kernel (8 mm full-width at half maximum).

Statistical analysis was based on a general linear model (GLM). Each condition was assigned a distinct regressor that was convolved with the hemodynamic response function. A high-pass filter with a cutoff-frequency of 1/256 Hz was applied to remove low frequency components. Serial autocorrelations were accounted for by modeling the error term as a first-order autoregressive process with a coefficient of 0.2. A second-level random effects analysis was run on the resulting individual whole-brain contrast images (canonical vs. scrambled biological motion). The group activation clusters ($p<0.05$, corrected for multiple comparisons) were assigned to the corresponding anatomical sites with the help of automated anatomical labeling (Tzourio-Mazoyer et al., 2002) including the 3D-MRI human cerebellar parcellation (Schmahmann et al., 1999), as implemented in SPM.

Functional connectivity analysis

The seed-voxel regression approach reveals which brain areas exhibit similar time courses as the seed region (Biswal et al., 1995). Regions of interest (ROIs) were selected in individual normalized functional data sets, with selection of the individual local maxima (for the contrast task vs. baseline; $p<0.001$, uncorrected) located closest to the group maxima for the two left cerebellar clusters. Crus I and VIIB ROIs were identified in all thirteen participants and subsequently overlaid on individual normalized structural images to control for location of the selected ROIs in the lobules Crus I and VIIB. For individual maxima in Crus I, *x*-coordinates ranged from −40 to −43, *y*-coordinates from −52 to −58, and *z*-coordinates from −29 to −34 (MNI space). Individual cluster sizes for Crus I varied from 832 to 1168 mm³. For individual maxima in VIIB, the ranges were from −33 to −38 for *x*-coordinates, from −63 to −69 for *y*-coordinates, and from −49 to −54 for *z*-coordinates. Cluster sizes of the corresponding ROIs ranged from 216 to 336 mm³. Average time courses from these two ROIs were extracted in each subject and included in individual whole-brain multiple regression analyses. To control for effects of physiological processes, six head motion parameters as well as time series from white matter and CSF masks derived from segmentation of the normalized structural images were included as covariates of no interest. Statistical inference was based on second-level random effects analysis of the contrast images resulting from individual regression.

Effective connectivity analysis

Subsequently, DCM was used to study effective connectivity between the left cerebellar Crus I and the right pSTS. DCM, as implemented in SPM8, allows studying task-dependent interactions between brain regions, based on their estimated neural activity (Friston et al., 2003; Stephan et al., 2010). The individual maxima closest to the group maxima for Crus I and pSTS were identified and regional time series were extracted as the first eigenvariate of all activated voxels (at a threshold of $p<0.001$, uncorrected) within an 8 mm radius of the individual maxima. The GLM created for the whole-brain analysis of the BOLD response was used as design matrix for DCM. Within-region coupling was modeled as recurrent self-connections (Friston et al., 2003), and visual input as reaching the pSTS. Fifteen different models with all possible types of interconnections between the pSTS and Crus I were constructed. The first three models assessed unidirectional communication from the pSTS to Crus I, either without any modulatory effects (model 1) or with modulation of this connection by processing of canonical (model 2) and scrambled biological motion (model 3). Model 4 assessed unidirectional communication from Crus I to the pSTS without modulatory effects. Modulation of this connection by canonical (model 5) and scrambled biological motion (model 6) were also considered. Bidirectional communication between the pSTS and Crus I was assessed in models 7–15. Model 7 did not include modulatory effects. Canonical biological motion modulated the connection from the pSTS to Crus I in model 8, and the connection from Crus I to the pSTS in model 9. Scrambled biological motion modulated the connection from the pSTS to Crus I in model 10, and the connection from Crus I to the pSTS in model 11. Both connections, from the pSTS to Crus I and from Crus I to the pSTS, were modulated either by canonical (model 12) or scrambled biological motion (model 13). Model 14 assessed modulatory effects of canonical biological motion on the connection from the pSTS to Crus I and of scrambled biological motion on the connection from Crus I to the pSTS. These modulatory effects were inverted in model 15. The models were compared by using fixed effects Bayesian model selection that provides negative free-energy values as an approximation to the log-evidences for the different models (Friston et al., 2007). Bayesian model selection favors models with both optimal fitting and complexity. Therefore, less complex models best explaining the observed data are preferred to apparently similar but less fitting and/or more complex models (Penny et al., 2004; Stephan et al., 2010). In order to obtain log-evidence differences required for model comparison, the log-evidence value of the least probable model (all three models 4–6 representing unidirectional communication from the Crus I to the pSTS were equally improbable) was subtracted from the log-evidence values of the other models. The optimal model was determined based on the greatest log-evidence difference. For the optimal model, Bayesian averaging was used to compute endogenous connectivity and modulatory parameters as well as their corresponding standard deviations and probabilities.

Results

fMRI brain activation during visual perception of body motion

In the fMRI whole-brain analysis, two regions in the left lateral cerebellum, the lobules Crus I ($x=-42$, $y=-56$, $z=-32$; MNI coordinates) and VIIB ($x=-36$, $y=-66$, $z=-52$), exhibited

increased response to human walking as compared to scrambled displays ($p<0.05$, corrected for multiple comparisons; Fig. 1). In agreement with earlier findings (e.g., Beauchamp et al., 2002, 2003; Gobbini et al., 2007; Grossman and Blake, 2002; Peelen et al., 2006; Pelphrey et al., 2003; Peuskens et al., 2005; Saygin et al., 2004; Vaina et al., 2001), increased activity was also observed in the right temporal cerebral cortex, including the fusiform gyrus, middle temporal cortex and the pSTS ($x=56$, $y=-50$, $z=10$). Detailed information on all activation clusters is represented in Table 1A.

Functional connectivity analysis

In order to explore left cerebellar engagement in the neural circuitry underpinning visual processing of biological motion, we conducted a seed-voxel functional connectivity analysis. This analysis indicated strongest functional connectivity between the left cerebellar lobule Crus I and the right pSTS ($x=58$, $y=-52$, $z=12$; $p<0.05$, corrected for multiple comparisons; see Fig. 2A). Other regions functionally connected with the left cerebellar lobule Crus I were the right orbitofrontal cortex, the right anterior superior temporal gyrus and the left medial frontal gyrus (see Table 1B). The functional connectivity analysis with a seed region in lobule VIIB did not yield significant results.

Effective connectivity analysis

DCM, as implemented in SPM8, was used to assess effective connectivity between the left cerebellar lobule Crus I and the right pSTS during visual processing of biological motion. Fifteen models including all possible types of communication between the pSTS and Crus I and modulatory effects of canonical or scrambled biological motion on these connections were designed and compared by using Bayesian model selection (see Methods Section Effective connectivity analysis and Fig. 3). This analysis indicated that model 9 with bidirectional communication between the left cerebellar lobule Crus I and the right pSTS, and specific modulation of the outgoing connection from Crus I to the pSTS by processing of canonical biological motion represented the optimal model (Fig. 2C). This model also was the most probable model at individual level. The log-evidence difference between this most probable and the next probable model (bidirectional communication between the pSTS and Crus I without modulatory effects, model 7) was 7.83. This log-evidence difference corresponds to a Group Bayes Factor of 2515. Bayes Factors higher than 150 are considered very strong evidence in favor of one model as compared to another (Penny et al., 2004). The endogenous connectivity parameters for model 9 were 0.55 ± 0.15 for Crus I-to-pSTS communication and 0.51 ± 0.18 for pSTS-to-Crus I communication with probabilities of 99% for both parameters. The parameter for modulation of the connection from Crus I to the pSTS by processing of canonical biological motion was 0.13 ± 0.02, with a probability of 98%.

Table 1
MNI coordinates, corresponding z-values and cluster sizes (in mm³) of (A) brain regions exhibiting activation during observation of biological motion displays, as compared with scrambled displays ($p<0.05$, corrected for multiple comparisons); and of (B) brain regions showing functional connectivity with the left cerebellar lobule Crus I in the seed-voxel regression analysis ($p<0.05$, corrected for multiple comparisons).

MNI coordinates					
Anatomical label	x	y	z	z-Value	Cluster size
A					
L cerebellum					
Lobule Crus I	−42	−56	−32	5.66	656
Lobule VIIB	−36	−66	−52	5.05	168
R posterior superior temporal sulcus (pSTS)	56	−50	10	5.49	856
R fusiform gyrus (FFG)					
Anterior	42	−42	−18	5.43	472
Posterior	46	−66	−18	5.91	2200
R middle temporal cortex	44	−74	4	5.18	1784
L middle temporal cortex	−52	−76	2	4.81	232
R medial frontal gyrus (MFG)					
Anterior	32	52	20	4.78	216
Posterior	36	−2	48	4.95	472
B					
R posterior superior temporal sulcus (pSTS)	58	−52	12	6.12	664
R orbitofrontal cortex	12	40	−14	5.93	528
R superior temporal gyrus (STG)	58	−12	−4	5.85	688
L medial frontal gyrus (MFG)	−38	44	22	5.72	376

Discussion

The outcome of the fMRI analysis indicates specific engagement of the left lateral cerebellum in visual processing of body motion. Two regions in the left lateral cerebellar lobules Crus I and VIIB exhibited increased activity to human biological motion as compared to scrambled displays. The lack of right cerebellar activity underlines the specificity of left cerebellar involvement in the network dedicated to visual processing of biological motion. A few earlier brain imaging PET (Bonda et al., 1996; Ptito et al., 2003) and 1.5T-fMRI (Grossman et al., 2000; Vaina et al., 2001) studies incidentally reported cerebellar activity during visual point-light biological motion tasks, and the findings are controversial as to cerebellar substructures that matter. Two regions in the left midline cerebellum exhibited higher PET activation elicited by point-light animals running versus drifting across the screen (Ptito et al., 2003). Increased left lateral cerebellar PET activation was found for point-light dance-like canonical as compared to scrambled displays (Bonda et al., 1996). Higher right midline cerebellar fMRI response was reported when contrasting canonical to scrambled point-light actions (jumping, kicking, running and throwing) during a one-back repetition task (Grossman et al., 2000). In the study by Vaina et al. (2001), in a two-alternative forced choice (2AFC) paradigm, five participants had to discriminate canonical from scrambled walkers or the global motion direction of the same stimuli. Elevated BOLD responses in both lateral cerebellar hemispheres were shown for the biological motion discrimination task, with canonical and scrambled point-light displays pooled together and contrasted against baseline. The left lateral cerebellar region QuP (posterior quadrangular lobule or lobule VI), more posterior and superior to the Crus I activation site in our study, was active during the biological motion but not a global motion task (Vaina et al., 2001). The present data carefully acquired in such a way that the most caudal parts of the cerebellum were covered in all participants, dovetail with recent findings on compromised visual sensitivity to human locomotion in patients with left cerebellar tumors. Patients with lesions to the left lateral cerebellum exhibit deficits in visual sensitivity to point-light body motion, whereas medial lesions do not substantially affect visual perception of human locomotion (Sokolov et al., 2010). Convergent evidence from lesion and brain imaging studies is essential for establishing reliable structure–function relationships.

The outcome of the study provides the first evidence in favor of bidirectional communication between the left lateral cerebellum and the right pSTS. Given limited knowledge on cerebro-cerebellar communication during biological motion processing, assessment of task-related functional connectivity primarily served as an initial step to identify candidate regions for subsequent DCM (Friston et al., 2011). While the outcome of the functional connectivity analysis may also reflect similar but not interdependent responses to biological motion in pSTS and Crus I, DCM allows studying task-dependent causal interactions between brain regions based on their estimated neural

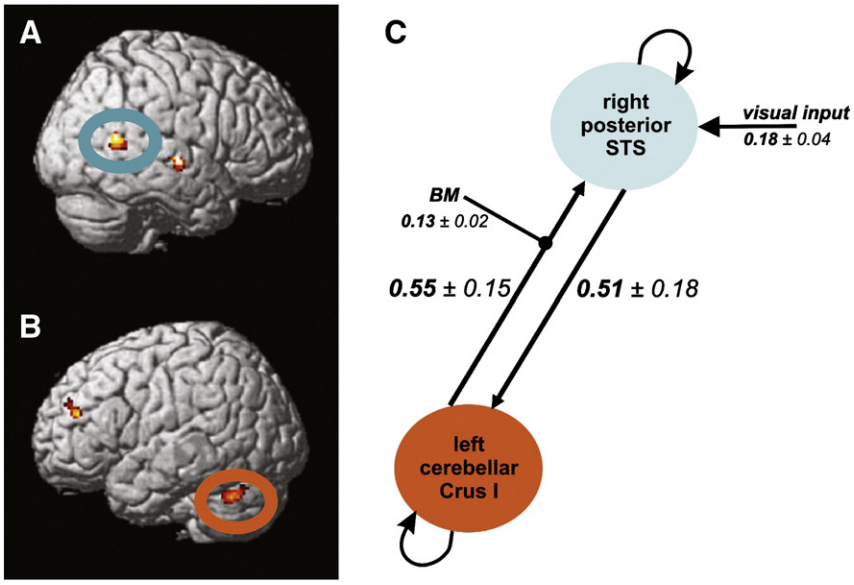

Fig. 2. Cerebro-cerebellar connectivity during observation of human locomotion. The seed-voxel regression analysis indicates significant interconnections ($p<0.05$, corrected for multiple comparisons) between the left cerebellar lobule Crus I and (A) the right posterior superior temporal sulcus (pSTS) and a more anterior region in the superior temporal gyrus, and (B) the left medial frontal gyrus. Activation overlaid on MNI 3D-template. (C) Dynamic causal modelling (DCM) points to reciprocal effective communication between the left cerebellar lobule Crus I and the right pSTS, with specific modulation of the outgoing connection from Crus I to the pSTS by biological motion (BM). Average endogenous connectivity and modulatory parameters, as well as their standard deviations are plotted next to the corresponding directions of communication.

activity (Friston et al., 2003) and indicates effective connectivity between these regions.

Neuroanatomical studies in non-human primates have separately assessed connections from the STS to the pons (Brodal, 1978; Glickstein et al., 1985; Schmahmann and Pandya, 1991) and from the pons to the cerebellum (Brodal, 1979). In non-human primates, the dorsal bank of the anterior STS hosts the equivalent of the human multisensory pSTS responding to biological motion (Bruce et al., 1981; Oram and Perrett, 1994; Perrett et al., 1985; Puce and Perrett, 2003). Lesions to both anterior and posterior portions of the rhesus monkey STS result in degeneration of dorsolateral pontine nuclei (Brodal, 1978), that are also the target of anterograde axonal transport of radioactive amino acids injected into the dorsal bank of the rhesus monkey STS (Schmahmann and Pandya, 1991). Findings in macaque monkeys on retrograde axonal transport of horseradish peroxidase from the dorsolateral pons to the dorsal bank of the medial STS further support these data (Glickstein et al., 1985).

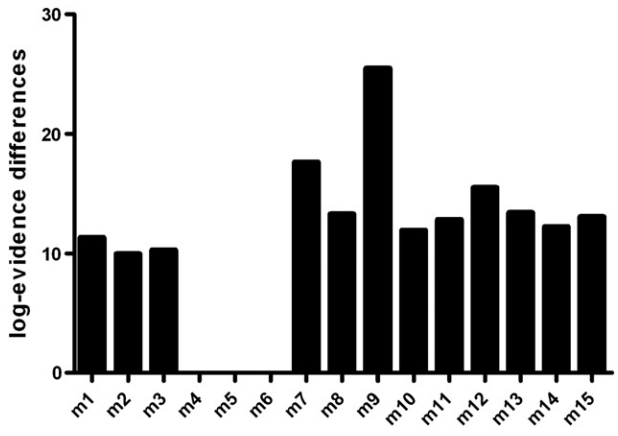

Fig. 3. Log-evidence differences for the 15 different models (m1–15) as provided by Bayesian model selection. To obtain log-evidence differences, the log-evidence values of the least probable models 4–6 were subtracted from the log-evidence values of the other models. This analysis indicates that model 9 (m9) with bidirectional communication between the posterior superior temporal sulcus (pSTS) and Crus I, and specific modulation of the outgoing connection from Crus I to the pSTS by canonical biological motion, is the most probable model with a log-evidence difference of 7.83 between m9 and the next probable model 7 (m7).

For the first time, the present work indicates that the left lateral cerebellum not only receives input from the right pSTS, but also modulates functional activity in the right pSTS. The findings suggest the existence of possible cerebellar projections to the STS, for which there has been a lack of experimental evidence. Modulation of the connection from the cerebellum to the pSTS by canonical biological motion emphasizes importance of this back projection specifically for processing of this kind of motion. Two recent resting state functional connectivity MRI (fcMRI) studies suggested that the superior temporal auditory areas are connected with the cerebellar lobules V and VI (O'Reilly et al., 2010), and the inferior temporal cortex is connected with the cerebellar lobules V, VI, and Crus I (Krienen and Buckner, 2009). In contrast to resting state fcMRI, the outcome of the present study indicates effective task-dependent connectivity between the right pSTS and the left cerebellar lobule Crus I during visual processing of body motion. The evidence for two-way communication between the right pSTS and the left lateral cerebellum parallels previous neuroanatomical findings on closed loops between the cerebellum and parietal, motor and frontal cortices (Strick et al., 2009). Yet, a similar pattern of structural connectivity between the temporal cortex and the cerebellum has not been shown. Presumably, high tract curvature may account for the failure of diffusion tensor imaging (DTI) to detect possible fiber tracts between the cerebellum and the STS (Ramnani et al., 2006). A further step toward uncovering cerebro-cerebellar connectivity would be a combination of fMRI with specific DTI sequences and algorithms.

Reciprocal interaction between the left cerebellum and the right STS has broad implications not only for cognitive, but also for clinical neuroscience. The STS is considered a cornerstone of the topographically overlapping brain networks subserving visual processing of biological motion and social cognition (Allison et al., 2000; Puce and Perrett, 2003; for recent review, see Pavlova, 2011). Deficient body motion processing in survivors of premature birth suffering from periventricular lesions (Pavlova et al., 2006, 2007; Taylor et al., 2009) may result from altered cerebro-cerebellar connectivity. Several neuropsychiatric conditions, such as ASD and schizophrenia are associated with impaired visual perception of body motion and

social cognition (Blake et al., 2003; Kim et al., 2005; Klin et al., 2009; Koldewyn et al., 2010). These disorders are also reported to be characterized by alterations in cerebro-cerebellar connectivity (Barnea-Goraly et al., 2004; Belmonte et al., 2004; Kanaan et al., 2009; Skudlarski et al., 2010). However, the two characteristic features of ASD and schizophrenia, namely compromised visual social perception and altered cerebro-cerebellar connectivity, have not yet been linked. This gap is narrowed by the present evidence for a functional loop between the left lateral cerebellum and the right pSTS, operating both in feedforward (the right pSTS to the left cerebellar lobule Crus I) and feedback directions during visual body motion processing. Recently reported lower fMRI response to biological motion in the right pSTS of autistic children (Kaiser et al., 2010) may be, at least to some extent, explained by deficient functioning within this loop in ASD. This proposal is in agreement with data in individuals with Asperger syndrome indicating that severity of social impairment correlates with the extent of structural alterations in the left superior cerebellar peduncle, the major output tract from the left cerebellum to the right cerebral cortex (Catani et al., 2008). These findings nicely dovetail with the present data indicating specific modulation of the output from the left cerebellar lobule Crus I to the right pSTS by processing of human locomotion.

Significance of the present findings may go beyond comprehension of a proper functioning of the neural circuitry dedicated to visual body motion processing. Through engagement in different functional neural networks, the STS is believed to subserve multimodal cognitive processing including audiovisual integration, face perception, social interaction and visual tasks on theory of mind (Beauchamp et al., 2004; Castelli et al., 2000; Hein and Knight, 2008; Howard et al., 1996; Pavlova et al., 2010; Pelphrey et al., 2005; Saxe et al., 2004; Schultz et al., 2005; Wyk et al., 2009). Recent fMRI data also indicate cerebellar involvement in audiovisual integration (Baumann and Greenlee, 2007; Baumann and Mattingley, 2010; Petrini et al., 2011). Brain imaging suggests involvement of the left lateral cerebellum in visual social cognition through body motion. Left lateral cerebellar activation is observed during recognition of dynamic, but not static, emotional facial expressions (Kilts et al., 2003), and perception of dynamic, as compared to static, emotional expressions of a full-light whole body (Grèzes et al., 2007). When observers reveal false intentions in others' actions, elevated fMRI response is found among other regions in the right pSTS and the left lateral cerebellum (Grèzes et al., 2004). In adults and 10-year-olds, both left lateral cerebellum and the right pSTS are active during visual processing of social interaction between moving geometric shapes in Heider-and-Simmel-like animations (Gobbini et al., 2007; Ohnishi et al., 2004). Further studies are needed to clarify whether the reciprocal connection between the left lateral cerebellar lobule Crus I and the right pSTS might also underpin social cognitive functions other than visual processing of body motion.

The present data shed light on the cerebellum as a well differentiated functional brain structure, and improve our understanding of cerebellar contribution to cognitive processing in normalcy and pathology. The findings open a window for further research on functional and structural connectivity between the cerebellum and the temporal cortex.

Supplementary materials related to this article can be found online at doi:10.1016/j.neuroimage.2011.08.039.

Acknowledgments

We thank Randolph Blake, Nikos Logothetis and Alex Martin for valuable comments on an earlier version of the manuscript, and Karl Friston and Klaas-Enno Stephan for their advice on dynamic causal modelling, and Marko Wilke for suggestions on connectivity analysis. We thank Alexander N. Sokolov for fruitful discussions. We are grateful to Jürgen Dax, Bernd Kardatzki, Gerd Pfister, Karsten Scheffler for technical support, Franziska Hösl, Albertine Stiens, Cornelia Veil for assistance with MRI scanning, and to the study participants. This work was supported by the Else Kröner Fresenius Stiftung (P63/2008 and 2010_A92), the Werner Reichardt Centre for Integrative Neuroscience Tübingen (project 2009-24), and by the Reinhold Beitlich Foundation to M.A.P. A.A.S was supported by a fellowship from the Integrated Graduate School of the Collaborative Research Center (SFB) 550 of the German Research Foundation (DFG) and by the Werner Reichardt Centre for Integrative Neuroscience Tübingen.

References

Allison, T., Puce, A., McCarthy, G., 2000. Social perception from visual cues: role of the STS region. Trends Cogn. Sci. 4, 267–278.
Barnea-Goraly, N., Kwon, H., Menon, V., Eliez, S., Lotspeich, L., Reiss, A.L., 2004. White matter structure in autism: preliminary evidence from diffusion tensor imaging. Biol. Psychiatry 55, 323–326.
Baumann, O., Greenlee, M.W., 2007. Neural correlates of coherent audiovisual motion perception. Cereb. Cortex 17, 1433–1443.
Baumann, O., Mattingley, J.B., 2010. Scaling of neural responses to visual and auditory motion in the human cerebellum. J. Neurosci. 30, 4489–4495.
Beauchamp, M.S., Lee, K.E., Argall, B.D., Martin, A., 2004. Integration of auditory and visual information about objects in superior temporal sulcus. Neuron 41, 809–823.
Beauchamp, M.S., Lee, K.E., Haxby, J.V., Martin, A., 2002. Parallel visual motion processing streams for manipulable objects and human movements. Neuron 34, 149–159.
Beauchamp, M.S., Lee, K.E., Haxby, J.V., Martin, A., 2003. FMRI responses to video and point-light displays of moving humans and manipulable objects. J. Cogn. Neurosci. 15, 991–1001.
Belmonte, M.K., Allen, G., Beckel-Mitchener, A., Boulanger, L.M., Carper, R.A., Webb, S.J., 2004. Autism and abnormal development of brain connectivity. J. Neurosci. 24, 9228–9231.
Biswal, B., Yetkin, F.Z., Haughton, V.M., Hyde, S., 1995. Functional connectivity in the motor cortex of resting human brain using echo-planar MRI. Magn. Reson. Imaging 34, 537–541.
Blake, R., Turner, L.M., Smoski, M.J., Pozdol, S.L., Stone, W.L., 2003. Visual recognition of biological motion is impaired in children with autism. Psychol. Sci. 14, 151–157.
Brodal, P., 1978. The corticopontine projection in the rhesus monkey: origin and principles of organization. Brain 101, 251–283.
Brodal, P., 1979. The pontocerebellar projection in the rhesus monkey: an experimental study with retrograde axonal transport of horseradish peroxidase. Neuroscience 4, 193–208.
Bruce, C., Desimone, R., Gross, C., 1981. Visual properties of neurons in a polysensory area in superior temporal sulcus of the macaque. J. Neurophysiol. 46, 369–384.
Bonda, E., Petrides, M., Ostry, D., Evans, A., 1996. Specific involvement of human parietal systems and the amygdala in the perception of biological motion. J. Neurosci. 16, 3737–3744.
Castelli, F., Happe, F., Frith, U., Frith, C., 2000. Movement and mind: a functional imaging study of perception and interpretation of complex intentional movement patterns. Neuroimage 12, 314–325.
Catani, M., Jones, D.K., Daly, E., Embiricos, N., Deeley, Q., Pugliese, L., Curran, S., Robertson, D., Murphy, D.G., 2008. Altered cerebellar feedback projections in Asperger syndrome. Neuroimage 41, 1184–1191.
Clower, D.M., West, R.A., Lynch, J.C., Strick, P.L., 2001. The inferior parietal lobule is the target of output from the superior colliculus, hippocampus, and cerebellum. J. Neurosci. 21, 6283–6291.
Cutting, J.E., 1978. Generation of synthetic male and female walkers through manipulation of a biomechanical invariant. Perception 7, 393–405.
Dum, R.P., Strick, P.L., 2003. An unfolded map of the cerebellar dentate nucleus and its projections to the cerebral cortex. J. Neurophysiol. 89, 634–639.
Friston, K.J., Li, B., Daunizeau, J., Stephan, K.E., 2011. Network discovery with DCM. Neuroimage 56, 1202–1221.
Friston, K., Mattout, J., Trujillo-Barreto, N., Ashburner, J., Penny, W., 2007. Variational free energy and the Laplace approximation. Neuroimage 34, 220–234.
Friston, K.J., Harrison, L., Penny, W., 2003. Dynamic causal modelling. Neuroimage 19, 1273–1302.
Glickstein, M., May III, J.G., Mercier, B.E., 1985. Corticopontine projection in the macaque: the distribution of labelled cortical cells after large injections of horseradish peroxidase in the pontine nuclei. J. Comp. Neurol. 235, 343–359.
Gobbini, M.I., Koralek, A.C., Bryan, R.E., Montgomery, K.J., Haxby, J.V., 2007. Two takes on the social brain: a comparison of theory of mind tasks. J. Cogn. Neurosci. 19, 1803–1814.
Grèzes, J., Fonlupt, P., Bertenthal, B., Delon-Martin, C., Segebarth, C., Decety, J., 2001. Does perception of biological motion rely on specific brain regions? Neuroimage 13, 775–785.
Grèzes, J., Frith, C.D., Passingham, R.E., 2004. Inferring false beliefs from the actions of oneself and others: an fMRI study. Neuroimage 21, 744–750.
Grèzes, J., Pichon, S., de Gelder, B., 2007. Perceiving fear in dynamic body expressions. Neuroimage 35, 959–967.
Grossman, E., Donnelly, M., Price, R., Pickens, D., Morgan, V., Neighbor, G., Blake, R., 2000. Brain areas involved in perception of biological motion. J. Cogn. Neurosci. 12, 711–720.
Grossman, E.D., Blake, R., 2002. Brain areas active during visual perception of biological motion. Neuron 35, 1167–1175.

Hein, G., Knight, R.T., 2008. Superior temporal sulcus—it's my area: or is it? J. Cogn. Neurosci. 20, 2125–2136.
Howard, R.J., Brammer, M., Wright, I., Woodruff, P.W., Bullmore, E.T., Zeki, S., 1996. A direct demonstration of functional specialization within motion-related visual and auditory cortex of the human brain. Curr. Biol. 6, 1015–1019.
Kaiser, M.D., Hudac, C.M., Shultz, S., Lee, S.M., Cheung, C., Berken, A.M., Deen, B., Pitskel, N.B., Sugrue, D.R., Voos, A.C., Saulnier, C.A., Ventola, P., Wolf, J.M., Klin, A., Vander Wyk, B.C., Pelphrey, K.A., 2010. Neural signatures of autism. Proc. Natl. Acad. Sci. U. S. A. 107, 21223–21228.
Kanaan, R.A., Borgwardt, S., McGuire, P.K., Craig, M.C., Murphy, D.G., Picchioni, M., Shergill, S.S., Jones, D.K., Catani, M., 2009. Microstructural organization of cerebellar tracts in schizophrenia. Biol. Psychiatry 66, 1067–1069.
Kilts, C.D., Egan, G., Gideon, D.A., Ely, T.D., Hoffman, J.M., 2003. Dissociable neural pathways are involved in the recognition of emotion in static and dynamic facial expressions. Neuroimage 18, 156–168.
Kim, J., Doop, M.L., Blake, R., Park, S., 2005. Impaired visual recognition of biological motion in schizophrenia. Schizophr. Res. 77, 299–307.
Klin, A., Lin, D.J., Gorrindo, P., Ramsay, G., Jones, W., 2009. Two-year-olds with autism orient to non-social contingencies rather than biological motion. Nature 459, 257–261.
Koldewyn, K., Whitney, D., Rivera, S.M., 2010. The psychophysics of visual motion and global form processing in autism. Brain 133, 599–610.
Krienen, F.M., Buckner, R.L., 2009. Segregated fronto-cerebellar circuits revealed by intrinsic functional connectivity. Cereb. Cortex 19, 2485–2497.
O'Reilly, J.X., Beckmann, C.F., Tomassini, V., Ramnani, N., Johansen-Berg, H., 2010. Distinct and overlapping functional zones in the cerebellum defined by resting state functional connectivity. Cereb. Cortex 20, 953–965.
Ohnishi, T., Moriguchi, Y., Matsuda, H., Mori, T., Hirakata, M., Imabayashi, E., Hirao, K., Nemoto, K., Kaga, M., Inagaki, M., Yamada, M., Uno, A., 2004. The neural network for the mirror system and mentalizing in normally developed children: an fMRI study. Neuroreport 15, 1483–1487.
Oram, M.W., Perrett, D.I., 1994. Responses of anterior superior temporal polysensory (STPa) neurons to "biological motion" stimuli. J. Cogn. Neurosci. 6, 99–116.
Pavlova, M.A., 2011. Biological motion processing as a hallmark of social cognition. Cereb. Cortex. doi:10.1093/cercor/bhr156.
Pavlova, M., Bidet-Ildei, C., Sokolov, A.N., Braun, C., Krägeloh-Mann, I., 2009. Neuromagnetic response to body motion and brain connectivity. J. Cogn. Neurosci. 21, 837–846.
Pavlova, M., Guerreschi, M., Lutzenberger, W., Krägeloh-Mann, I., 2010. Social interaction revealed by motion: dynamics of neuromagnetic gamma activity. Cereb. Cortex 20, 2361–2367.
Pavlova, M., Lutzenberger, W., Sokolov, A., Birbaumer, N., 2004. Dissociable cortical processing of recognizable and non-recognizable biological movement: analysing gamma MEG activity. Cereb. Cortex 14, 181–188.
Pavlova, M., Lutzenberger, W., Sokolov, A.N., Birbaumer, N., Krägeloh-Mann, I., 2007. Oscillatory MEG response to human locomotion is modulated by periventricular lesions. Neuroimage 35, 1256–1263.
Pavlova, M., Marconato, F., Sokolov, A., Braun, C., Birbaumer, N., Krägeloh-Mann, I., 2006. Periventricular leukomalacia specifically affects cortical MEG response to biological motion. Ann. Neurol. 59, 415–419.
Pavlova, M., Staudt, M., Sokolov, A., Birbaumer, N., Krägeloh-Mann, I., 2003. Perception and production of biological movement in patients with early periventricular brain lesions. Brain 126, 692–701.
Peelen, M.V., Wiggett, A.J., Downing, P.E., 2006. Patterns of fMRI activity dissociate overlapping functional brain areas that respond to biological motion. Neuron 49, 815–822.
Pelphrey, K.A., Mitchell, T.V., McKeown, M.J., Goldstein, J., Allison, T., McCarthy, G., 2003. Brain activity evoked by the perception of human walking: controlling for meaningful coherent motion. J. Neurosci. 23, 6819–6825.
Pelphrey, K.A., Morris, J.P., Michelich, C.R., Allison, T., McCarthy, G., 2005. Functional anatomy of biological motion perception in posterior temporal cortex: an fMRI study of eye, mouth and hand movements. Cereb. Cortex 15, 1866–1876.
Penny, W.D., Stephan, K.E., Mechelli, A., Friston, K.J., 2004. Comparing dynamic causal models. Neuroimage 22, 1157–1172.
Perrett, D.I., Smith, P.A.J., Mistlin, A.J., Chitty, A.J., Head, A.S., Potter, D.D., Broennimann, R., Milner, A.D., Jeeves, M.A., 1985. Visual analysis of body movements by neurones in the temporal cortex of the macaque monkey: a preliminary report. Behav. Brain Res. 16, 153–170.
Petersen, S.E., Fox, P.T., Posner, M.I., Mintun, M., Raichle, M.E., 1989. Positron emission tomographic studies of the processing of single words. J. Cogn. Neurosci. 1, 153–170.
Petrini, K., Pollick, F.E., Dahl, S., McAleer, P., McKay, L., Rocchesso, D., Waadeland, C.H., Love, S., Avanzini, F., Puce, A., 2011. Action expertise reduces brain activity for audiovisual matching actions: an fMRI study with expert drummers. Neuroimage 56, 1480–1492.
Peuskens, H., Vanrie, J., Verfaillie, K., Orban, G.A., 2005. Specificity of regions processing biological motion. Eur. J. Neurosci. 21, 2864–2875.
Ptito, M., Faubert, J., Gjedde, A., Kupers, R., 2003. Separate neural pathways for contour and biological-motion cues in motion-defined animal shapes. Neuroimage 19, 246–252.
Puce, A., Perrett, D., 2003. Electrophysiology and brain imaging of biological motion. Philos. Trans. R. Soc. B: Biol. Sci. 358, 435–445.
Ramnani, N., Behrens, T.E., Johansen-Berg, H., Richter, M.C., Pinsk, M.A., Andersson, J.L., Rudebeck, P., Ciccarelli, O., Richter, W., Thompson, A.J., Gross, C.G., Robson, M.D., Kastner, S., Matthews, P.M., 2006. The evolution of prefrontal inputs to the cortico-pontine system: diffusion imaging evidence from Macaque monkeys and humans. Cereb. Cortex 16, 811–818.
Saxe, R., Xiao, D.K., Kovacs, G., Perrett, D.I., Kanwisher, N., 2004. A region of right posterior temporal sulcus responds to observed intentional actions. Neuropsychologia 42, 1435–1446.
Saygin, A.P., Wilson, S.M., Hagler Jr., D.J., Bates, E., Sereno, M.I., 2004. Point-light biological motion perception activates human premotor cortex. J. Neurosci. 24, 6181–6188.
Schmahmann, J.D., Doyon, J., McDonald, D., Holmes, C., Lavoie, K., Hurwitz, A.S., Kabani, N., Toga, A., Evans, A., Petrides, M., 1999. Three-dimensional MRI atlas of the human cerebellum in proportional stereotaxic space. Neuroimage 10, 233–260.
Schmahmann, J.D., Pandya, D.N., 1991. Projections to the basis pontis from the superior temporal sulcus and superior temporal region in the rhesus monkey. J. Comp. Neurol. 308, 224–248.
Schultz, J., Friston, K.J., O'Doherty, J., Wolpert, D.M., Frith, C.D., 2005. Activation in posterior superior temporal sulcus parallels parameter inducing the percept of animacy. Neuron 45, 625–635.
Skudlarski, P., Jagannathan, K., Anderson, K., Stevens, M.C., Calhoun, V.D., Skudlarska, B.A., Pearlson, G., 2010. Brain connectivity is not only lower but different in schizophrenia: a combined anatomical and functional approach. Biol. Psychiatry 68, 61–69.
Sokolov, A.A., Gharabaghi, A., Tatagiba, M.S., Pavlova, M., 2010. Cerebellar engagement in an action observation network. Cereb. Cortex 20, 486–491.
Stephan, K.E., Penny, W.D., Moran, R.J., den Ouden, H.E., Daunizeau, J., Friston, K.J., 2010. Ten simple rules for dynamic causal modelling. Neuroimage 49, 3099–3109.
Strick, P.L., Dum, R.P., Fiez, J.A., 2009. Cerebellum and nonmotor function. Annu. Rev. Neurosci. 32, 413–434.
Taylor, N.M., Jakobson, L.S., Maurer, D., Lewis, T.L., 2009. Differential vulnerability of global motion, global form, and biological motion processing in full-term and preterm children. Neuropsychologia 47, 2766–2778.
Tzourio-Mazoyer, N., Landeau, B., Papathanassiou, D., Crivello, F., Etard, O., Delcroix, N., Mazoyer, B., Joliot, M., 2002. Automated anatomical labeling of activations in SPM using a macroscopic anatomical parcellation of the MNI MRI single-subject brain. Neuroimage 15, 273–289.
Vaina, L.M., Solomon, J., Chowdhury, S., Sinha, P., Belliveau, J.W., 2001. Functional neuroanatomy of biological motion perception in humans. Proc. Natl. Acad. Sci. U. S. A. 98, 11656–11661.
Wyk, B.C., Hudac, C.M., Carter, E.J., Sobel, D.M., Pelphrey, K.A., 2009. Action understanding in the superior temporal sulcus region. Psychol. Sci. 20, 771–777.